# Non-symmetric spin-pumping in a multiferroic heterostructure

Pauline Rovillain, Ronei Cardoso de Oliveira, Massimiliano Marangolo, Jean-Yves Duquesne

# Non-symmetric spin-pumping in a multiferroic heterostructure

Pauline Rovillain,[1,*] Ronei Cardoso de Oliveira,[2] Massimiliano Marangolo,[1] and Jean-Yves Duquesne[1]

[1] *Sorbonne Université, CNRS, Institut des NanoSciences de Paris, INSP, UMR7588, F-75005 Paris, France*
[2] *Laboratório de Nanoestruturas para Sensores, Universidade Federal do Paraná, Curitiba 81531-990, PR, Brazil*

(Dated: March 19, 2020)

We present spin pumping experiments in Co/Pt bilayers, using surface acoustic waves to induce the magnetization precession. We show that the substrate on which the bilayer is deposited plays a role in the spin current excitation/detection processes. The electrical polarization of the substrate breaks the invariance for an inversion of both the magnetization vector and acoustic wave vector.

From its early beginning, spintronics research concentrated its efforts on handling spin polarization current due to an imbalance of spin-up and spin-down conductive electrons, leading to the success-story of giant magnetic resistance spin valves[1–3]. More recently, pure spin currents, i.e. a spin flux without charge flux, are at the centre of interest since they do not give rise to Oersted field and more important, they do not produce Joule heating, reducing power dissipation in spintronics devices, as in STT-MRAM[4–6]. These applications require an increase in the emission and detection efficiencies via a full understanding of the complex physics behind pure spin currents. Spin current can be detected by inverse spin Hall effect (ISHE) that corresponds to the conversion of a spin current into a detectable charge current by measuring the voltage on a normal metal (NM) presenting a strong spin-orbit interaction (e.g. Pt). Concerning pure spin current emission different tools have been proposed in litterature. Emission can be obtained by temperature gradients through the spin Seebeck effect[7–9], by charge currents (spin Hall effect[10]) and by magnetization dynamics (spin pumping[9,11,12]). This last mechanism permits to generate pure spin current via ferromagnetic resonance (FMR) in a ferromagnetic material (FM), leading to spin accumulation in an adjacent non magnetic material. Generally, FMR is obtained by radio-frequency (RF) electromagnetic means or by RF currents[13]. Interestingly, FMR and spin pumping has also been triggered by acoustic means taking advantage of resonant magnetoelastic coupling (MEC) in a Co/Pt bilayer[11]. Here, mature surface acoustic wave (SAW) technology is used to drive the dynamics of magnetization of a thin Co film, in the GHz regime and by a remote, non inductive and no dissipation tool. This is the so-called SAW-FMR that is obtained when the SAW frequency matches the magnetization precession frequency of the FM under a uniform magnetic field. Indeed, it has been shown in Ni[14], (Ga,Mn)(As,P)[15] and Fe[16] that the SAW creates an effective RF field which excites the uniform magnetization precession mode of the ferromagnetic layer. This precession pumps a spin current into the NM layer[17]. In turn, this spin current generates an electric field ($\mathbf{E}_{\mathrm{ISHE}}$) in the NM layer through the ISHE: $\mathbf{E}_{\mathrm{ISHE}} \sim \mathbf{J}_S \times \boldsymbol{\sigma}$ where $\mathbf{J}_S$ is the spin-current density and $\boldsymbol{\sigma}$ correspond to the spin polarization vector. This electric field is converted into a measurable voltage $V_I$ between both ends of the Pt strip.

The main purpose of this letter is to investigate the impact of some symmetry rules on the spin-pumping excitation/detection process. In particular, we have performed experiments to compare the spin pumping excitation/detection efficiency when the directions of the magnetization ($\mathbf{M}$) and the directions of the acoustic wave vector ($\mathbf{k_{SAW}}$) are reversed. We report a peculiar behaviour of SAW-FMR assisted spin pumping in a multiferroic system where a FM/NM (Co/Pt) bilayer is in contact with a ferroelectric (FE) substrate ($LiNbO_3$) as respect to the simultaneous $\mathbf{M}$ and $\mathbf{k_{SAW}}$ directions inversion operation. We suggest that the remanent electrical polarization vector affects the ISHE voltage.

Figure 1(a) is a sketch of the samples. We used two types of substrates: $LiNbO_3$ and $Al_2O_3$. $LiNbO_3$ is not centrosymmetric (space group is $R3m$). It is ferroelectric and therefore piezoelectric. $Al_2O_3$ is centrosymmetric (space group is $R\bar{3}m$). It is neither piezoelectric nor ferroelectric. The $LiNbO_3$ substrate is an Y-cut plate and we propagate SAW, on the free surface, along its Z-axis. It is also well-known that the Z-axis is the direction of the spontaneous electrical polarization $\mathbf{P}$[18,19] and we verified that our $LiNbO_3$ substrate is a single-domain ferroelectric, using polarized light microscopy. The $Al_2O_3$ substrate is a (0001)-cut plate and we propagate SAW, on the free surface, along the Y-axis. The orientations of the two substrates have been verified by XRD. On both substrates we call $x$ the SAW propagation axis, oriented from interdigitated transducer (IDT1) to the other (IDT2). We also define an in-plane oriented axis $x'$ at an angle $\phi$ from $x$. We apply a magnetic field $\mathbf{B_{ext}}$ along $x'$ (see Fig.1(a)). On both substrates, a $500\,\mu\mathrm{m} \times 1.5\,\mathrm{mm}$ bi-layer of Co (10 nm) and Pt (7 nm) is deposited by electron beam evaporation at the center.

SAW bursts are emitted and detected electrically by means of two nominally identical IDTs made by electronic lithography symmetrically with respect to the Co/Pt strip. In the case of the $LiNbO_3$/Co/Pt sample, IDTs are deposited directly onto the piezoelectric substrate. However, in case of the $Al_2O_3$/Co/Pt sample, a thin ZnO piezoelectric layer is deposited on the surface, under the IDTs areas, so as to emit SAWs. 200ns SAW bursts are emitted at 1.5 and 1.3 GHz for $LiNbO_3$ and $Al_2O_3$ respectively. Bursts electrical incident power is 19 dBm (79 mW), except for power study in Fig 2.

The DC spin current is detected via the ISHE in the Pt

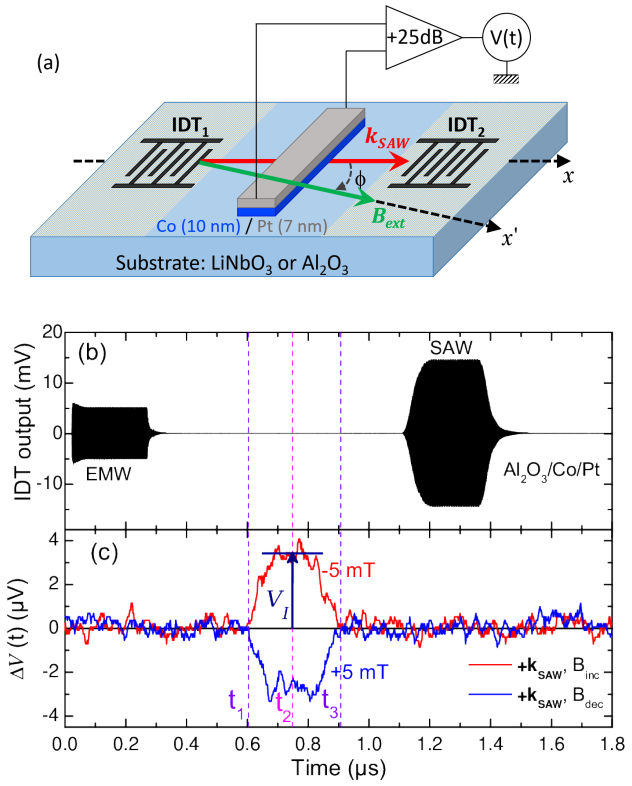


FIG. 1. (a) Sketch of the sample: Co(10nm)/Pt(7nm) bilayers on $LiNbO_3$ or $Al_2O_3$ substrate. For $Al_2O_3$ substrate a ZnO piezoelectric layer is deposited under the IDTs (light green area). IDTs have 30 pairs of fingers. Aperture is 500 $\mu$m. Made in Al with a ratio of 0.5. $x$ axis is parallel to $\mathbf{k_{SAW}}$, oriented from IDT1 towards IDT2. $x'$ axis is at an angle $\phi$ relative to $x$. An in-plane external magnetic field $\mathbf{B_{ext}}$ is applied along $x'$. An amplifier recovers the spin current signal $V(t)$. (b) Acoustic signal recorded by the output IDT as a function of time. EMW signal and SAW pulses are observed. (c) Spin current signal recorded for the $Al_2O_3$/Co/Pt sample for $\mathbf{k_{SAW}}$ configuration in increasing ($B_{\rm inc}$) and decreasing field ($B_{\rm dec}$). $\Delta V(t, B_{\rm ext}) = V(t, B_{\rm ext}) - V(t, B_{\rm ref})$ where $V$ is the spin current signal. $B_{\rm ext} = \pm 5$ mT. $B_{\rm ref} = \pm 35$ mT. At $t_2$, $\Delta V(t_2, B_{\rm ext})$ shows a change of sign by a reversal of $\mathbf{B_{ext}}$.

layer by measuring the time-dependent voltage between both ends of the Co/Pt bi-layer with a DC-amplifier (bandwidth = 0-20 MHz, gain = 25 dB, input and output impedance = 50 Ω). The output voltage $V(t)$ is recorded synchronously with the acoustic bursts (see Fig.1). To separate, in the time domain, the spin current signal $V$ from the electromagnetic wave (EMW) and from the acoustic (SAW) signals, the distances between each IDT and the bi-layer is carefully designed (1.25 and 2.25 mm for $LiNbO_3$ and $Al_2O_3$, respectively). In an experimental run, we record $V(t)$ as a function of the applied field amplitude, at a given orientation $\phi$. The initial amplitude $B_{\rm sat}$ is set to saturate the magnetic film. Then, the amplitude either increases ($B_{\rm inc}$) from -35 mT to +35 mT ($B_{\rm sat}$ = -350 mT) or decreases ($B_{\rm dec}$) from +35 mT to -35 mT ($B_{\rm sat}$ = +350mT).

These measurements were performed for various orientation $\phi$ and also for opposite acoustic wave vectors $\mathbf{k_{SAW}}$. The direction of $\mathbf{k_{SAW}}$ is reversed by connecting the input signal to one IDT or to the other. Since the ITDs are symmetrical with respect to the Co/Pt strip, spin pumping occurs in the same time range $[t_1, t_3]$ for both propagation directions.

From the magnetic point of view, each evaporated Co layer has different characteristics. We performed longitudinal magneto-optical Kerr (MOKE) measurements to record the magnetic cycle $M/M_S(B)$ (not shown here). These measurements gave the coercive field $B_c$. The magnetic cycle is obtained for different $\phi$ angles in different compounds. In this paper, we choose to present the results obtained for two specific samples where $B_c$ is lower than the resonant field $B_{\rm res}$. From broadband-FMR (BB-FMR) measurements between 2.5 and 8.5 GHz, we record the FMR frequency, $F_{\rm FMR}$, as a function of the in-plane magnetic field amplitude ($B_{\rm ext}$)[20]. By extrapolation of our experimental values ($F_{\rm FMR}$ vs $B_{\rm ext}$) using the Kittel formula[21] on both Co/Pt samples, we found a SAW-FMR resonance condition around 4 mT. Both samples $Al_2O_3$/Co/Pt/ and $LiNbO_3$/Co/Pt are invariant by a rotation of $\pi$, regarding their MOKE magnetic cycles.

To investigate the impact of the symmetry rules on the spin-pumping excitation/detection process, we have performed spin pumping measurement on Co/Pt bilayers deposited on two different substrates $Al_2O_3$ and $LiNbO_3$. First, we present our results. Afterward, we will analyse them in term of symmetries.

Measurements, presented here, have been performed at $\phi = 60°$ with $B_c = 3$ mT for $Al_2O_3$ and $\phi = 0°$ with $B_c = 1.1$ mT for $LiNbO_3$. Figure 1(c) shows the spin current signal $\Delta V(t) = V(t, B_{\rm ext}) - V(t, B_{\rm ref})$ for $Al_2O_3$/Co/Pt, $B_{\rm ext} = \pm 5$ mT and $B_{\rm ref} = \pm 35$ mT. This substraction is performed to eliminate spurious deterministic signals. According to calculation, no SAW-FMR and no spin pumping are expected at ±35 mT. On the contrary, at $B_{\rm ext} = \pm 5$ mT, the acoustic frequency matches the precession frequency of the uniform mode. Hence, when the acoustic burst goes through the Co/Pt bi-layer, in the time range $[t_1,t_3]$ ([0.6-0.9] $\mu$s in the case of the $Al_2O_3$/Co/Pt sample), it induces the ferromagnetic resonance of Co and a pure spin current is launched in the adjacent Pt layer, with a maximum value around $t_2$. The magnitude of the spin current is proportional to the time-averaged value $V_I$ of $\Delta V(t)$, around $t_2$ (between 0.7 and 0.8 $\mu$s for $Al_2O_3$/Co/Pt).

Maximum spin currents (in absolute value) are measured at the resonance fields, $B_{\rm res}$ (see Fig. 4). We observe the change of sign of $V_I$ with the reversal of $\mathbf{M}$, induced by the reversal of $\mathbf{B}_{\rm ext}$ (since $B_c < B_{\rm res}$), which is a necessary condition for acoustic spin pumping[22]. We also note that $V_I$ (proportional to the spin current) is proportional to the incident electrical power ($P_{el}$), and then to the electrical power injected in the IDT, as shown in Fig.2 for $Al_2O_3$. The same behavior is observed for

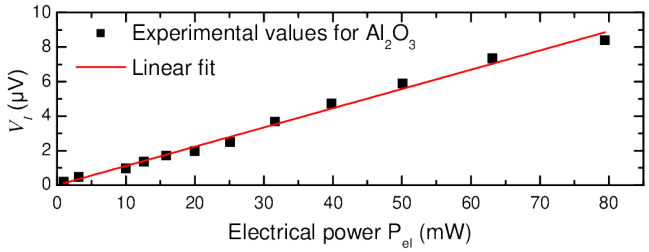


FIG. 2. $V_I$ (proportional to the spin current amplitude) as function of incident electrical power on IDT for $Al_2O_3$/Co/Pt sample. The red line is a linear fit, in good agreement, with the data[23].

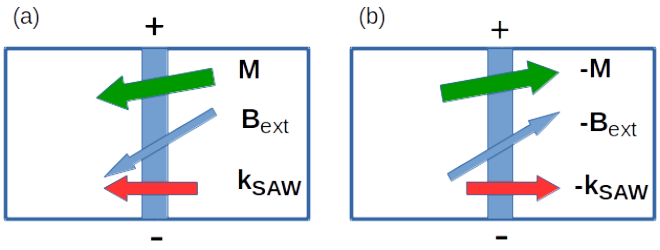


FIG. 3. Sketch of the sample (substrate and bilayer). (a) and (b) display two configurations of in-plane external magnetic field $\mathbf{B_{ext}}$, magnetization $\mathbf{M}$ and $\mathbf{k_{SAW}}$. (b) is obtained from (a) by inversion of $\mathbf{B_{ext}}$, $\mathbf{M}$ and $\mathbf{k_{SAW}}$. The voltage is measured between the (+) and (-) terminals.

$LiNbO_3$ sample. Indeed, this is in good agreement with experiments of K.Ando *et al.*[12] and equations details by F.Czeschka *et al.*[22]: $V_I \propto \sin^2\theta_{\rm res}$ where $\theta_{\rm res}$ is the magnetic precession cone angle at resonance. Assuming a small precession angle : $\sin\theta_{\rm res}^2 \propto \theta_{\rm res}^2$. Moreover $\theta_{\rm res}$ is proportional to the effective microwave magnetic field $h_{\rm mw}$ induced by SAW, which is proportional to the strain $\varepsilon$. Then, $V_I \propto \theta_{\rm res}^2 \propto h_{\rm mw}^2 \propto \varepsilon^2$. Furthermore, $\varepsilon^2$ is proportional to the electrical power $P_{\rm el}$ so that $V_I \propto P_{\rm el}$.

At first glance, our results on $V_I$ vs $\mathbf{B}_{\rm ext}$ seem to be similar to those obtained by M.Weiler *et al*[11]. However, a first difference is observed in our measurements at the coercive fields. Indeed, a current is emitted at $-B_c$ and $+B_c$ for decreasing and increasing field, respectively. The origin of this current is not yet understood and is beyond the scope of this paper. However, since $B_c$ is more or less close to the resonant field, the current superimposes on the spin current and it becomes difficult to separate the two contributions. This is the reason why, not to be disturbed by an additional signal, we have chosen in this paper to present spin current measurements $V_I$ for low coercive field samples and, in particular, at angles where $B_{\rm c}$ is the weakest.

So, let us now see what is expected when the magnetic field and the acoustic wave vector are reversed. Figure 3 displays sketches of a sample (substrate and bi-layer) subject to two configurations (a) and (b), regarding the orientations of in-plane applied field $\mathbf{B_{ext}}$, magnetization $\mathbf{M}$ and acoustic wave vector $\mathbf{k_{SAW}}$. Configuration (b) is obtained from (a) by reversing $\mathbf{B_{ext}}$, $\mathbf{M}$ and $\mathbf{k_{SAW}}$. However, if the whole sample, including both substrate and bi-layer, is invariant by a rotation of $\pi$, configuration (b) can also be obtained from (a) by combining a rotation of $\pi$ and an exchange of the (+) and (-) terminals. Therefore, if the sample is invariant by a rotation of $\pi$, we infer that going from (a) to (b) will change the sign of the measured voltage between the (+) and (-) terminals but not its magnitude. Conversely, if the measured voltage between the (+) and (-) terminals have either the same sign or different amplitudes, then the sample is not invariant by a rotation of $\pi$.

To test the previous conclusions, we chose two substrates which are not invariant by a rotation of $\pi$, about an axis perpendicular to the propagation plane. In $Al_2O_3$, the symmetry about (0001) is only of order 3. However, a $2\pi/6$ rotation leaves unchanged the location of the oxygen atoms and only involves a change in the orientation of the aluminium triangles which are located between the oxygen planes. Therefore, in our $Al_2O_3$/Co/Pt sample, the non-invariance by a rotation of $\pi$ is somehow "weak" since it is just due to slight variations of atoms stacking. In $LiNbO_3$, the $\pi$ rotation about the Y-axis reverses the orientation of the permanent ferroelectric polarization (parallel to Z). Therefore, in our $LiNbO_3$/Co/Pt sample, the non-invariance by a rotation of $\pi$ is not only due to stacking but also to the presence of an electric polarization vector. This is a "strong" non-invariance.

From an experimental point of view, reversing $\mathbf{k_{SAW}}$ and $\mathbf{B_{ext}}$ is quite easy. However, reversing $\mathbf{M}$ is a little bit more tricky because of memories effects associated with the magnetic hysteresis. If configuration (a) is reached from a positive saturating field ("decreasing field scan"), configuration (b) must be reached from a negative saturating field ("increasing field scan"), and conversely. To conclude, in order to check the symmetry rules, we should compare the voltages measured either for [$\mathbf{k_{SAW}}$, $\mathbf{B_{ext}}$, $B_{\rm dec}$] and [$-\mathbf{k_{SAW}}$, $-\mathbf{B_{ext}}$, $B_{\rm inc}$], or for [$\mathbf{k_{SAW}}$, $\mathbf{B_{ext}}$, $B_{\rm inc}$] and [$-\mathbf{k_{SAW}}$, $-\mathbf{B_{ext}}$, $B_{\rm dec}$]. From a practical point of view, the comparison can be easily done. For example, let us consider two field scans: [$\mathbf{k_{SAW}}$, $B_{\rm inc}$] and [$-\mathbf{k_{SAW}}$, $B_{\rm dec}$]. For the first scan, we plot the voltage $V_I$ versus the signed amplitude of the field. For the second scan, we plot the opposite voltage $-V_I$ versus the opposite of the signed amplitude of the field. Due to previous symmetry considerations, both curves could eventually not superimpose. The same conclusion is valid when comparing two other field scans: [$\mathbf{k_{SAW}}$, $B_{\rm dec}$] and [$-\mathbf{k_{SAW}}$, $B_{\rm inc}$].

Fig.4 (a,b) displays our results for the $LiNbO_3$/Co/Pt sample. Clearly, the curves obtained for [$\mathbf{k_{SAW}}$, $B_{\rm dec}$] and [$-\mathbf{k_{SAW}}$, $B_{\rm inc}$] scans (or [$\mathbf{k_{SAW}}$, $B_{\rm inc}$] and [$-\mathbf{k_{SAW}}$, $B_{\rm dec}$] scans) do not superimpose. For example, at $B_{\rm ext} =$ 5 mT, the magnitude of the voltage is either 2.5 or 5 $\mu$V, depending on the scans. This factor of 2 cannot be attributed to possible different intensities of the acoustic field, at $\mathbf{k_{SAW}}$ and $-\mathbf{k_{SAW}}$, arising from different effi-

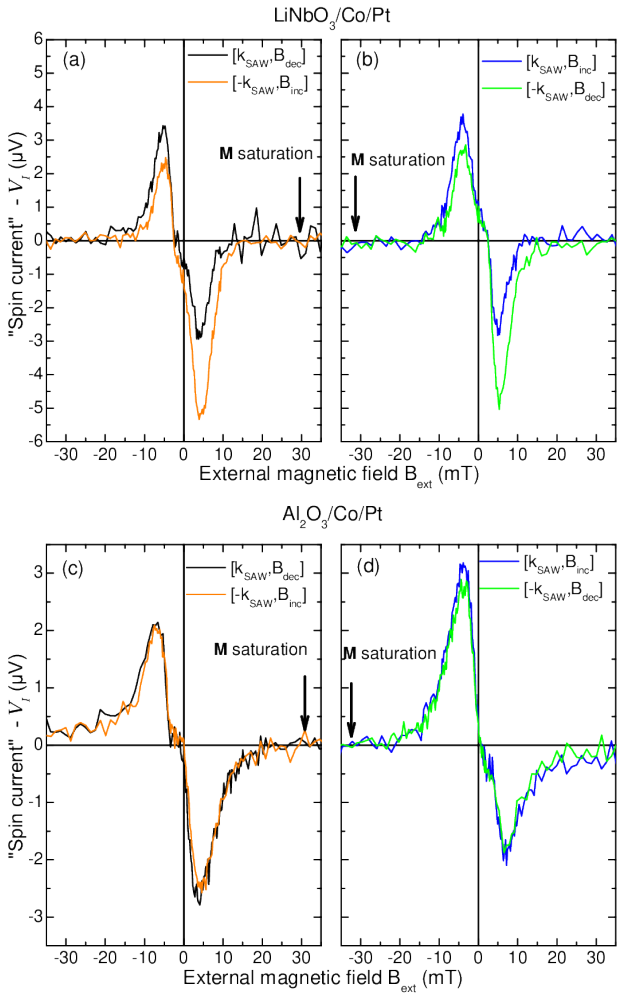


FIG. 4. (a, b) Co/Pt on $LiNbO_3$ and (c, d) Co/Pt on $Al_2O_3$. $V_I$ (proportional to the spin current) versus $B_{ext}$ after symmetry operations on $-\mathbf{k_{SAW}}$ scans. Black and blue curves: raw data. Orange and green curves: starting from raw data, $V_I$ and $B_{ext}$ are multiplied by -1 (see main text). (a, c) Comparison between [$\mathbf{k_{SAW}}$, $B_{dec}$] and [$-\mathbf{k_{SAW}}$, $B_{inc}$]. (b, d) Comparison between [$\mathbf{k_{SAW}}$, $B_{inc}$] and [$-\mathbf{k_{SAW}}$, $B_{dec}$].

ciencies of the IDT1 and IDT2 transducers. If a multiplying factor were applied to correct the amplitudes at 5 mT, then the difference in amplitudes at -5 mT would further increase. We conclude that the breaking of the $\pi$ rotational symmetry due to the permanent ferroelectric polarization $\mathbf{P}$ seems to have a strong effect on spin-pumping. We observed this for all angles $\phi$ and samples studied even if $B_c > B_{res}$. This phenomenon must not be confused with "non-reciprocal" acoustic propagation observed in magnetic materials where only $\mathbf{k_{SAW}}$is inverted[24].

Fig.4 (c,d) displays our results for the $Al_2O_3$/Co/Pt sample. The curves obtained for corresponding field scans superimpose. Reversing simultaneously $\mathbf{k_{SAW}}$, $\mathbf{B_{ext}}$ and $\mathbf{M}$ changes the sign of the measured voltage but not its magnitude. Indeed, slightly different amplitudes are observed which can be attributed to different intensities of the acoustic field, at $\mathbf{k_{SAW}}$ and $-\mathbf{k_{SAW}}$, arising from different efficiencies of the two transducers. The same multiplying factor of 1.1 can be applied to correct the amplitudes at 5 mT and at -5 mT. We conclude that the "weak" breaking of the $\pi$ rotational symmetry has no measurable effect on spin-pumping.

In $LiNbO_3$/Co/Pt sample, the origin of the effect has to be determined. One possibility concerns the excitation process and involves a coupling between the ferroelectric polarization $\mathbf{P}$ of $LiNbO_3$ and the ferromagnetic moment of Co, as for magnetoelectric materials[25] or for artificial composite multiferroic systems[26]. This could modify either the magnetic precession cone angle at resonance, or the magnetic precession frequency, or both, and then modify the spin current generation. Nevertheless the Broad-Band-FMR measurements that we performed did not permit to point out any resonance shift after magnetic field reversal. This may indicate that spin-pumping is much more sensitive to interface magneto-electric effects. Other processes involving the detection can be excluded since the electrical field in the Pt layer, arising from $\mathbf{P}$, must be very weak, because of the geometry and of screening effects. Moreover, the electrical field would be directed normal to $\mathbf{E}_{\mathrm{ISHE}}$ and could not contribute to the measured current. It would have been interesting to quantify the effect of electrical polarization on spin current generation by modifying or reversing $\mathbf{P}$ through the application of an electric field. Unfortunately, the fields required to reverse the polarization are beyond our technical capabilities. Indeed, the coercive electric field of the $LiNbO_3$ is $E_c > 210$ kV.cm$^{-1}$ which would require to apply on our samples a field[27] $E > 21$ kV.

In conclusion, we have investigated the acoustic spin pumping in Co/Pt bilayers deposited on $LiNbO_3$ and $Al_2O_3$ substrates. Our experiments pinpoint the breaking of a rotational symmetry that we attribute to the permanent electrical polarization of $LiNbO_3$. We suggest that this polarization is an important factor in the spin pumping excitation processes. The nature of the coupling with the magnetic polarization is still unclear. It may be due to a magnetoelectric coupling at the interface between $LiNbO_3$ and Co. It will be interesting to use an easy commutable ferroelectric substrate to manipulate $\mathbf{P}$ in order to modify the emission of spin current. This observation gives the opportunity to use a new approach to increase the spin current with a clear generation process as SAW-FMR.

## ACKNOWLEDGMENTS

The authors acknowledge L.Becerra and M.Rosticher for optical and electronic lithography, S.Suffit for e-beam evaporation of Co/Pt bilayers, F.Vidal for assistance during MOKE experiments, Y.J. Zheng for X-ray diffraction measurements and C.Gourdon and L.Thevenard for careful reading.

* pauline.rovillain@insp.upmc.fr


[1] M. N. Baibich, J. M. Broto, A. Fert, F. N. Van Dau, F. Petroff, P. Eitenne, G. Creuzet, A. Friederich, and J. Chazelas, Phys. Rev. Lett. **61**, 2472 (1988).

[2] G. Binasch, P. Grünberg, F. Saurenbach, and W. Zinn, Phys. Rev. B **39**, 4828 (1989).

[3] J. M. George, L. G. Pereira, A. Barthélémy, F. Petroff, L. Steren, J. L. Duvail, A. Fert, R. Loloee, P. Holody, and P. A. Schroeder, Phys. Rev. Lett. **72**, 408 (1994).

[4] S. Maekawa, S. O. Valenzuela, E. Saitoh, and T. Kimura, Spin Current (Oxford University Press, 2017) pp. 1–520.

[5] L. Berger, Phys. Rev. B **54**, 9353 (1996).

[6] A. Makarov, T. Windbacher, V. Sverdlov, al, K. L. Wang, J. G. Alzate, and P. Khalili Amiri, J. Phys. D: Appl. Phys **46**, 74003 (2013).

[7] K. Uchida, S. Takahashi, K. Harii, J. Ieda, W. Koshibae, K. Ando, S. Maekawa, and E. Saitoh, Nature **455**, 778 (2008).

[8] K. Uchida, J. Xiao, H. Adachi, J. Ohe, S. Takahashi, J. Ieda, T. Ota, Y. Kajiwara, H. Umezawa, H. Kawai, G. E. Bauer, S. Maekawa, and E. Saitoh, Nature Materials **9**, 894 (2010).

[9] M. Matsuo, Y. Ohnuma, T. Kato, and S. Maekawa, Phys. Rev. Lett. **120**, 037201 (2018).

[10] T. Kimura, Y. Otani, T. Sato, S. Takahashi, and S. Maekawa, Phys. Rev. Lett. **98**, 156601 (2007).

[11] M. Weiler, H. Huebl, F. S. Goerg, F. D. Czeschka, R. Gross, and S. T. B. Goennenwein, Phys. Rev. Lett. **108**, 176601 (2012).

[12] K. Ando, S. Takahashi, J. Ieda, Y. Kajiwara, H. Nakayama, T. Yoshino, K. Harii, Y. Fujikawa, M. Matsuo, S. Maekawa, and E. Saitoh, J. Appl. Phys **109**, 103913 (2011).

[13] A. Okada, Y. Takeuchi, K. Furuya, C. Zhang, H. Sato, S. Fukami, and H. Ohno, PR Applied **12**, 014040 (2019).

[14] M. Weiler, L. Dreher, C. Heeg, H. Huebl, R. Gross, M. S. Brandt, and S. T. Goennenwein, Phys. Rev. Lett. **106**, 117601 (2011).

[15] L. Thevenard, I. S. Camara, S. Majrab, M. Bernard, P. Rovillain, A. Lemaître, C. Gourdon, and J.-Y. Duquesne, Phys. Rev. B **93** (2016).

[16] J.-Y. Duquesne, P. Rovillain, C. Hepburn, M. Eddrief, P. Atkinson, A. Anane, R. Ranchal, and M. Marangolo, PR Applied **12**, 024042 (2019).

[17] H. Adachi and S. Maekawa, Solid State Communications **198**, 22 (2014).

[18] K. Nassau, H. J. Levinstein, and G. M. Loiacono, Journal of Physics and Chemistry of Solids **27**, 983 (1966).

[19] K. Nassau, H. J. Levinstein, and G. M. Loiacono, Journal of Physics and Chemistry of Solids **27**, 989 (1966).

[20] A. B. Hamida, S. Sievers, K. Pierz, and H. W. Schumacher, J. Appl. Phys. **114**, 123704 (2013).

[21] C. Kittel, J. Phys. Radium **12**, 291 (1951).

[22] F. D. Czeschka, L. Dreher, M. S. Brandt, M. Weiler, M. Althammer, I.-M. Imort, G. Reiss, A. Thomas, W. Schoch, W. Limmer, H. Huebl, R. Gross, and S. T. B. Goennenwein, Phys. Rev. Lett. **107**, 046601 (2011).

[23] The power dependence measurement is performed for $\phi = 50^\circ$ to get high $V_I$ intensity and the possibility to recover the signal at low power. The current emitted at $B_c$ is also higher but does not disturb the measurement.

[24] R. E. Camley, Surface Science Reports **7**, 103 (1987).

[25] J. P. Velev, S. S. Jaswal, and E. Y. Tsymbal, Philosophical Transactions of the Royal Society A: Mathematical, Physical and Engineering Sciences **369**, 3069 (2011).

[26] N. Jedrecy, H. J. von Bardeleben, V. Badjeck, D. Demaille, D. Stanescu, H. Magnan, and A. Barbier, Phys. Rev. B **88**, 121409(R) (2013).

[27] S. Kim, V. Gopalan, and A. Gruverman, Appl. Phys. Lett. **80**, 2740 (2002).